UDK 620.1:67.017:669.245:539.377
Original scientific article/Izvirni znanstveni članek

ISSN 1580-2949
MTAEC9, 53(5)671(2019)

EFFECT OF SOLUTION TREATMENT ON GAMMA-PRIME RECOVERY IN A CREEP-DAMAGED DIRECTIONALLY SOLIDIFIED Ni SUPERALLOY

VPLIV RAZTOPNEGA ŽARJENJA NA POPRAVO FAZE γ' V DIREKTNO STRJENI IN ZARADI LEZENJA POŠKODOVANI Ni SUPERZLITINI

Junfeng Xiao, Wenshu Tang*, Qing Nan, Sifeng Gao, Yongjun Li, Jiong Zhang

Xi'an Thermal Power Research Institute Co., Ltd., 99 Yanxiang Road, Xi'an, China

Prejem rokopisa – received: 2019-02-20; sprejem za objavo – accepted for publication: 2019-03-27

doi:10.17222/mit.2019.046

The effect of different solution conditions on the γ' phase of a creep-damaged DZ411 superalloy during a process combining hot isostatic pressing (HIP) and re-heat rejuvenation was investigated. The analysis results showed that proper solution temperature and time are necessary for dissolving coarsened and rafted γ' precipitates, allowing the optimum reprecipitation of the γ' precipitates during the following aging, avoiding incipient melting. It was also found that a higher solution temperature results in a smaller size and lower volume fraction of the γ' precipitates. A two-hour solution treatment is enough to complete the dissolving of the remnant primary γ' precipitates and produce unimodal spheroidal secondary γ' precipitates. High cooling rates after the solution treatment give rise to finer and more secondary γ' precipitates. The complete re-heat rejuvenation procedure including a full solution and two-step aging can produce duplex-sized γ' precipitates including coarse cubic γ' precipitates and fine spherical γ' precipitates, endowing the superalloy with excellent high-temperature creep properties. It was verified that the γ' precipitate morphology and creep properties of the creep-damaged DZ411 superalloy can be restored with a simple re-heat rejuvenation process.

Keywords: directionally solidified superalloys, creep damage, re-heat rejuvenation, γ' precipitates

Avtorji so raziskovali učinek različnih raztopnih žarjenj na fazo γ' v vroče izostatsko stiskani (HIP) superzlitini DZ411. Zlitina je bila po izdelavi med postopkom lezenja poškodovana in renovirana (mikrostrukturno obnovljena) s postopkom ponovnega segrevanja. Rezultate so primerjali tudi z zlitino, ki ni bila HIP-ana. Rezultati analiz so pokazali, da je za raztapljanje grobih in ?naplavljenih? γ' izločkov potrebno raztopno žarjenje pri primerno visoki temperaturi in ustreznem času zadrževanja na tej temperaturi. To zagotavlja optimalno ponovno izločanje med naslednjim staranjem brez nataljevanja. Prav tako so ugotovili, da višja temperatura raztopnega žarjenja povzroča manjše γ' izločke in njihov manjši volumski delež. Dvourno raztopno žarjenje zadostuje za popolno raztapljanje primarnih γ' izločkov in tvorbo enomodalnih krogličnih sekundarnih γ' izločkov. Večje hitrosti ohlajanja po raztopnem žarjenju povzročajo nastanek finejših in večje število sekundarnih γ' izločkov. Popolna prenova poškodovane superzlitine s ponovnim segrevanjem vključuje popolno raztapljanje in dvostopenjsko staranje (izločevalno utrjevanje), kar povzroča nastanek dvojne velikosti faze γ' z grobimi kubičnimi in finimi krogličnimi γ' izločki. Takšna mikrostrukturno prenovljena superzlitina ima odlično visokotemperaturno odpornost proti lezenju. Avtorji so dokazali, da je možno morfologijo γ' izločkov in odpornost superzlitine DZ411 proti lezenju po njeni poškodbi z lezenjem popolnoma restavrirati z enostavnim ponovnim procesom poprave oz. segrevanja.

Ključne besede: direktno strjena superzlitina, poškodbe zaradi lezenja, raztopno žarjenje. poprava, γ' izločki

1 INTRODUCTION

Turbine blades are one of the most important hot-section-path (HGP) components realizing energy transformation in modern gas-turbine systems. Due to the complex service conditions including high temperature, high stress, corrosion and oxidation environment, turbine blades, after a long-term service exposure, inevitably suffer from microstructural damage, such as rafting or coarsening of γ' precipitates, all of which have a detrimental effect on the blade performance.[1,2] Therefore, it is necessary to regularly replace or refurbish turbine blades. However, turbine blades require the application of superalloy materials, air cooling, thermal-barrier coating and other advanced technologies. The complexity of the production process and the addition of high-cost refractory elements make the production cost of the blades higher and higher. The high cost of new replacement components provided a strong incentive for developing proper refurbishment procedures as economical methods to extend the service lives of blades.[3,4]

Rejuvenation heat treatments, including a simple re-heat rejuvenation treatment or recovery cycles incorporating both hot isostatic pressing (HIP) and heat treatment, were developed as a critical step in the refurbishment of degraded blades.[5,6] Previously, many studies about the recovery of the material microstructure in thermally exposed blades with an equiaxed structure had been conducted.[7–18] Subsequently, the HIP process was incorporated in the rejuvenation heat treatment of Inconel X-750 in 1977.[8] The early work consistently

*Corresponding author's e-mail:
tangwenshu@tpri.com.cn

showed that heat treatments alone could substantially recovery the material microstructure and that an additional benefit was achieved through the HIP process for the rejuvenation cycle in some instances.[9,10] Although subsequent studies reached mixed conclusions regarding the effectiveness of HIP recovery cycles, with some authors concluding that it is effective,[11,12] and others concluding that it is not,[13,14] there is still a common view that the HIP process has a positive impact on healing creep cavities and casting shrinkage porosity, and that heat treatment can effectively improve the microstructure and properties.[15,16]

At present, HIP recovery cycles are successfully used in the refurbishment and lifetime extension of degraded HGP components, applying a variety of equiaxed cast superalloys such as Udimet 500, Nimonic 115, Nimonic 263, IN738, GTD 111, Hastelloy X, FSX 414, and a few directionally solidified superalloys.[13,17–21] However, in the case of serviced components without any creep voids, HIP has no obvious benefit.[16] In fact, many directionally solidified superalloys are resistant to creep voids due to the minimum number of oriented grain boundaries, which indicates that they are likely to require the use of simple re-heat rejuvenation treatment consisting only of solution and aging treatments, which is a cheaper method for recovering the microstructure and properties of a directionally solidified superalloy.[16,22,23] For the re-heat rejuvenation treatment, the solution conditions intensely affect γ' precipitation characteristics. Meanwhile, an improper solution treatment may cause undesirable effects, such as incipient melting or recrystallization, especially for directionally solidified or single-crystal superalloys.

To explore application possibility for simple re-heat rejuvenation treatment in recovering the microstructure of a service-damaged directionally solidified superalloy, we conducted a recovery study on the DZ411 superalloy,[24] placing emphasis on the effects of different solution conditions on the γ' precipitate characteristic of the creep-damaged DZ411 superalloy during a re-heat rejuvenation process in this work. Finally, the recovery degree of the microstructure and creep properties of the creep-damaged DZ411 superalloy after a completed rejuvenation procedure was evaluated.

2 EXPERIMENTAL PART

Cylindrical bars of directionally solidified DZ411 superalloy, 12 mm in diameter and 200 mm in length, were produced under a vacuum atmosphere using the high-rate solidification method.[25] Before this, the DZ411 master alloy needed to be melted in a vacuum-induction furnace. The chemical composition of the superalloy was Ni-13.6Cr-9.14Co-4.9Ti-2.97Al-3.44W-1.6Mo-2.87Ta-0.09C-0.01B (*w*/%), as determined with an Axios Max X-ray fluorescence spectrometer, iCAP6300 optical emission spectroscopy and AA600 atomic absorption. In the present investigation, after the heat treatment, the DZ411 superalloy was considered as the original superalloy.

Standard creep specimens of the DZ411 superalloy were taken from the original superalloy. Crystal orientations of creep specimens were analyzed with the Laue X-ray back-reflection method, and crystal orientation deviations were controlled within 10° from the [001] orientation. In order to simulate the creep damage of turbine blades during a long-term service, interrupted creep tests of the DZ411 superalloy were performed on an RDJ50 creep testing machine with a furnace attachment at 980 °C and 190 MPa. Interruption points at the secondary stage of creep were chosen based on creep-rupture curves. The DZ411 superalloy after the interrupted creep test was considered as the damaged superalloy in the present investigation.

The damaged superalloy was then subjected to different heat-treatment cycles under an argon atmosphere in order to restore the degraded microstructure. The effects of the crucial solution-treatment parameters including temperature, holding time and cooling rate on the microstructure of the DZ411 superalloy were investigated. Detailed heat-treatment schedules are listed in **Table 1**. In order to prevent the superalloy samples from oxidizing during the heat-treatment process, the damaged superalloy was first sealed in a quartz tube filled with argon before it was place into the furnace.

The metallographic samples were prepared by sectioning, grinding, polishing and etching with a solution of 10 g of copper sulfate in 50 mL of hydrochloric acid and 50 mL of water. The microstructures of all the samples were examined with a PMG3 optical microscope (OM) and JSM-6460 scanning electron microscopy (SEM). Quantitative analyzing of the microstructures was conducted on the SEM micrographs using the Image Tool software as a semi-quantitative image analyzer. Since the quantitative metallographic investigation is principally a statistical measurement, many images of different conditions were analyzed. However, only one image from each set is shown in the present study as the representative one.

Table 1: Re-heat treatment schedules for the creep-damaged DZ411 superalloy

Cycle	Full solution			Partial solution			Aging		
	T (°C)	*t* (h)	Cooling	*T* (°C)	*t* (h)	Cooling	*T* (°C)	*t* (h)	Cooling
A	1180	2	AC	-	-	-	-	-	-
B	1200	2	AC	-	-	-	-	-	-
C	1220	2	AC	-	-	-	-	-	-
D	1240	2	AC	-	-	-	-	-	-
E	1220	1	AC	-	-	-	-	-	-
F	1220	3	AC	-	-	-	-	-	-
G	1220	4	AC	-	-	-	-	-	-
H	1220	2	FC	-	-	-	-	-	-
I	1220	2	AC	1121	2	AC	843	24	AC

Note: AC – air cooling, FC – furnace cooling

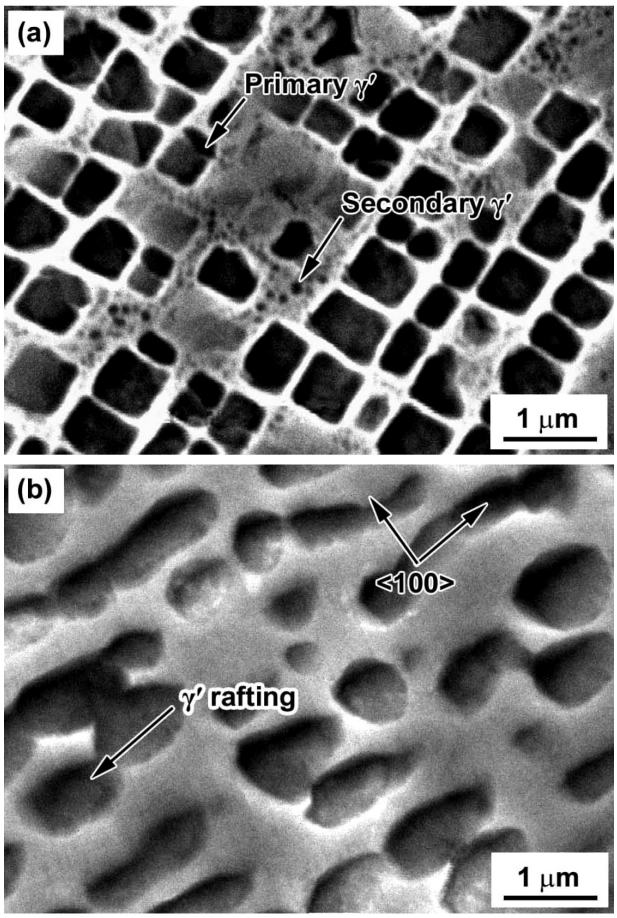

Figure 1: γ' precipitate microstructure for the original and damaged superalloy

3 RESULTS AND DISCUSSION

3.1 Original and creep-damaged microstructures

The microstructures of the original and damaged superalloy are shown in **Figure 1**. As can be observed in **Figure 1a**, the microstructure of the original superalloy exhibits a bimodal distribution of coarse primary γ' precipitates and fine secondary γ' precipitates within the austenitic γ matrix. The primary γ' precipitates, with the average size of 0.6 μm and a volume fraction of 50.3 %, have a cubic morphology, while the secondary γ' precipitates, with the average size of 0.11 μm and a volume fraction of 2.49 %, have a spherical morphology. However, the γ' precipitates of the damaged superalloy lost their original morphology (as shown in **Figure 1b)**. In particular, the primary γ' precipitates are coarsened and converted into spheroidal ones at the expense of the fine secondary γ' precipitates, resulting in a sharp decrease in the secondary γ' precipitates. It is believed that the coarsening of the γ' precipitates in nickel-based superalloys is in accordance with the Ostwald ripening mechanism, according to the Lifshitz-Slyozov-Wagner theory and subsequent modifications,[26] and that the coarsening process of the primary γ' precipitates is driven by the reduction in the total interfacial energy. **Table 2** summarizes the statistical data of the γ' precipitate characteristics for different states of the superalloy. It can also be seen that the volume fraction of the primary γ' precipitates of the damaged superalloy decreased significantly compared with that of the original superalloy.

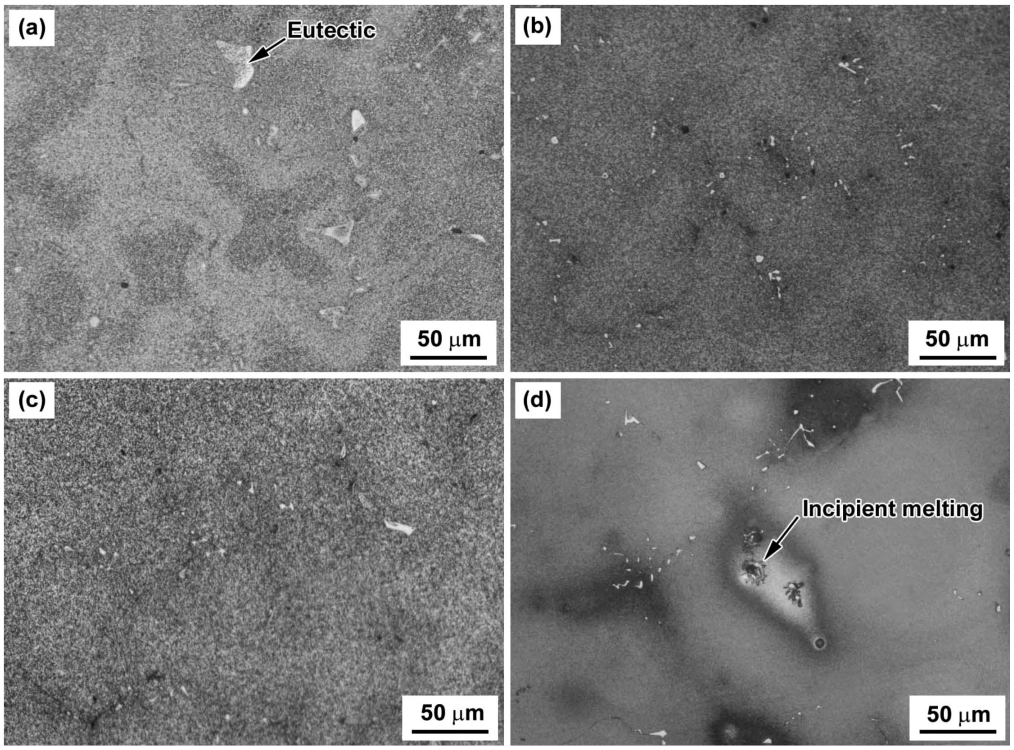

Figure 2: Optical micrographs of the damaged superalloy after solution treatments at: a) 1180 °C, b) 1200 °C, c) 1220 °C and d) 1240 °C

3.2 Microstructure after various solution-treatment schedules

To determine the proper solid solution temperature, various solution treatments were initially performed on the damaged superalloy at four holding temperatures (1180, 1200, 1220 and 1240) °C for 2 h and subsequently cooled in air to room temperature (corresponding to heat-treatment cycles A–D), respectively. Optical micrographs of the superalloy after the solution treatments at different holding temperatures are shown in **Figure 2**. It is clearly seen that the size of γ-γ' eutectic decreased as the solution temperature increased from 1180 °C to 1240 °C. However, when the solution treatment was performed at 1240 °C, incipient melting in the interdendritic region occurred and the γ-γ' eutectic phase almost disappeared. Therefore, 1240 °C is the solidus temperature of the damaged superalloy.

Figure 3 shows the γ' precipitate microstructure of the damaged superalloy after the solution treatment at different holding temperatures (1180, 1200, 1220 and 1240) °C for 2 h and subsequent air cooling to room temperature (heat treatment cycles A–D, respectively). The measured size and volume fraction of the γ' precipitates in the damaged superalloy before and after different heat-treatment cycles are presented in **Table 2**. It is obvious that the obtained γ' precipitates, except for heat-treatment cycle A, lost their rafting and coarsening characteristics. As seen in **Figure 3a**, it is clear that the 1180 °C/2 h/AC solution treatment (heat-treatment cycle A) gave rise to a decrease in the size and volume fraction of the γ' precipitates and produced a nearly bimodal, spheroidal γ' microstructure with coarse and fine γ' precipitates within the austenitic γ matrix, compared with the γ' precipitates in the damaged superalloy. In fact, 1180 °C is the subsolvus temperature for the γ' precipitate dissolution in the DZ411 superalloy. It indicates that a partial dissolution of the coarsened prime γ' precipitates in the damaged superalloy occurred. A large number of undissolved prime γ' precipitates, namely the remnant prime γ' precipitates, are retained in the matrix. Meanwhile, a partial dissolution of the prime γ' precipitates incorporated more solute atoms into the γ matrix, leading to the formation of fine secondary γ' precipitates, namely cooling precipitates, in the space between the remnant ones. Hence, it can be concluded that the coarse prime γ' precipitates are the remnant prime γ' precipitates and the finer ones are the secondary γ' precipitates that formed during the cooling process after the solution treatment.

However, when the solution temperature increased up to 1200 °C (heat-treatment cycle B), the γ' precipitates lost the entire rafted and coarsened morphology and exhibited a smaller size and a nearly unimodal, spheroidal microstructure (shown in **Figure 3b)**, compared with the γ' precipitates in the damaged superalloy. The formation of unimodal, spheroidal γ' precipitates implies that almost a complete dissolution of the remnant prime γ' precipitates occurred after heat-treatment cycle B. It can be deduced that the formed unimodal, spheroidal γ' precipi-

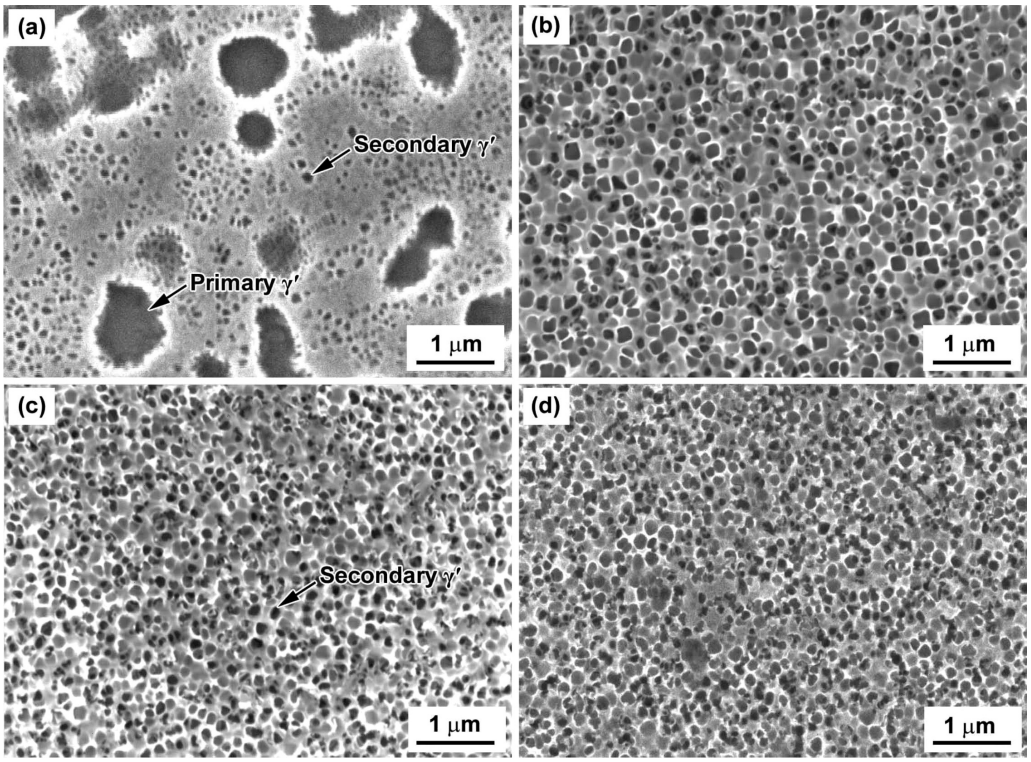

Figure 3: γ' precipitate microstructure of the damaged superalloy after different solution temperatures and cooling rates: a) Sample A (1180 °C/2 h, air cooling), b) Sample B (1200 °C/2 h, air cooling), c) Sample C (1220 °C/2 h, air cooling), d) Sample D (1240 °C/2 h, air cooling)

tates are almost the secondary γ' precipitates. As the solution temperature further increased up to 1220 °C (heat-treatment cycle C) and 1240 °C (solution-heat treatment cycle D), the secondary γ' precipitates were still nearly unimodal and spheroidal, exhibiting a slight decrease in the size and an increase in the volume fraction (see **Figures 3c** and **3d** and **Table 2**). It is believed that further dissolution of the remnant prime γ' precipitates at a higher solution temperature incorporated more solute into the matrix, resulting in finer secondary precipitates being formed during the cooling process after the solution treatment. In view of the fact that the solution treatment at 1240 °C caused incipient melting, the suitable solution temperature is determined to be 1220 °C for the re-heat rejuvenation treatment of the creep-damaged DZ411 superalloy.

Besides the solid-solution temperature, the holding time and cooling rate are also important factors, influencing the γ' precipitate characteristics. The γ' precipitate microstructure of the damaged superalloy after the solution treatment at 1220 °C for different holding times (1, 3 and 4) h and the subsequent air cooling to room temperature (corresponding to heat-treatment cycles E–G) are shown in **Figure 4a** to **4c**, respectively. Compared with the γ' precipitates obtained after heat-treatment cycle C, it is seen that as the holding time increased from 1 h to 2 h, all the γ' precipitates exhibited a similar unimodal, spheroidal microstructure and also a slight increase in the volume fraction, indicating that the holding time of 1 h at the solution temperature of 1220 °C is not enough to dissolve the remnant prime γ' precipitates. However, as the holding time further increased up to 3 h (heat-treatment cycle F) and 4 h (heat-treatment cycle G), the γ' precipitates showed a slight increase in the average size and squareness, and also a slight decrease in the volume fraction, possibly resulting from the contribution of the elastic strain energy during the solution treatments.[27] **Figure 4d** represents the γ' precipitate microstructure produced after heat-treatment cycle H, in which the cooling from the solution temperature to room temperature is performed by the furnace.

Comparing the γ' precipitate microstructures obtained after heat-treatment cycles C and H, it can be easily found that heat-treatment cycle H produces a lower density and large cubes of the γ' precipitates, unlike the finer, unimodal, spheroidal γ' precipitates obtained after heat-treatment cycle C (**Figure 3c**). This can be related to the cooling rate during the cooling process after the solution treatment. During the furnace cooling, the nucleation rate of the γ' precipitates is expected to be lower; meanwhile, a longer time is available for the diffusion of solute atoms and growth of the precipitates due to the low cooling rate.[28] However, according to the statistical parameters for the γ' precipitates after cycles C and H (**Table 2**), it is to be noted that the volume fractions of the γ' precipitates after cycles C and H are almost the same, indicating that the γ' precipitates grow slowly due to the solute ejection from the matrix during slow cooling, partially compensating for the advantage of the high γ' nucleation rate caused by air cooling.

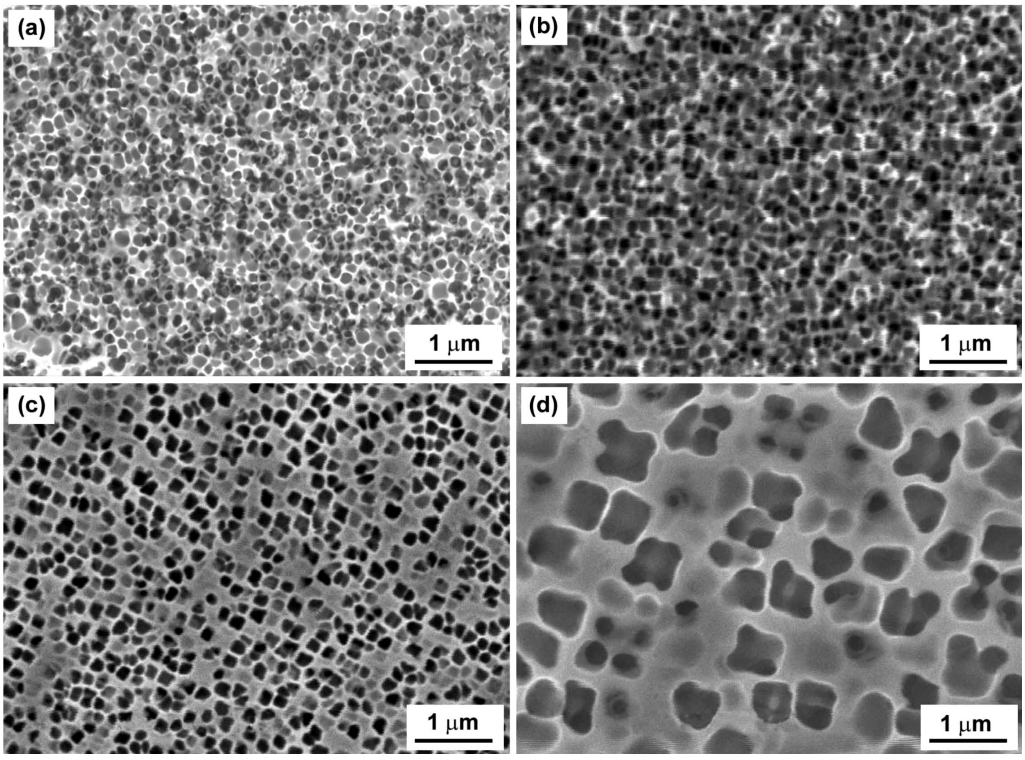

Figure 4: γ' precipitate microstructure of the damaged superalloy after different solution times and cooling rates: a) Sample E (1220 °C/1 h, air cooling), b) Sample F (1220 °C/3 h, air cooling), c) Sample G (1220 °C/4 h, air cooling), d) Sample H (1220 °C/2 h, furnace cooling)

Table 2: Statistical data for the γ' precipitate characteristic parameters for the damaged and rejuvenated superalloy

Condition	γ' type	Average size /μm	Volume fraction /%
Original superalloy	Primary γ' Secondary γ'	0.600±0.029 0.105±0.022	50.325±0.221 2.486±0.006
Damaged superalloy	Primary γ' Secondary γ'	0.800±0.032 -	37.495±0.462 -
A	Primary γ' Secondary γ'	0.696±0.079 0.101±0.025	25.221±0.816 11.442±0.007
B	Primary γ' Secondary γ'	- 0.292±0.032	- 39.480±0.020
C	Primary γ' Secondary γ'	- 0.154±0.013	- 40.140±0.023
D	Primary γ' Secondary γ'	- 0.147±0.026	- 41.95±0.013
E	Primary γ' Secondary γ'	- 0.151±0.019	- 38.587±0.018
F	Primary γ' Secondary γ'	- 0.162±0.028	- 40.931±0.282
G	Primary γ' Secondary γ'	- 0.169±0.017	- 37.854±0.281
H	Primary γ' Secondary γ'	- 0.586±0.049	- 40.966±0.416
I	Secondary γ' Tertiary γ'	0.394±0.042 0.071±0.003	42.510±0.200 6.488±0.004

3.3 Microstructure and creep properties of the rejuvenated superalloy

Due to a lack of a complete rejuvenation procedure, a single solution treatment could not fully recover the microstructure of the damaged superalloy, achieving its original state. **Figure 5** shows the γ' precipitate microstructure of the damaged superalloy after a complete re-heat rejuvenation procedure consisting of a full solution and two-step aging at the following conditions: 1220 °C/2 h/AC + 1121 °C/2h/AC + 843 °C/24 h/AC (heat treatment cycle I). It is obvious that heat-treatment cycle I produced a duplex-size γ' precipitate microstructure with coarse cubic γ' precipitates and fine spherical γ' precipitates, which are analogous to those of the original superalloy except for the smaller γ' precipitates. Especially the size of the coarse γ' precipitates is larger

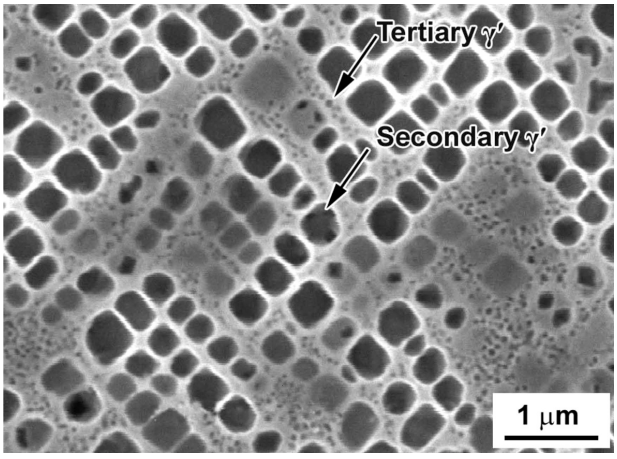

Figure 5: γ' precipitate microstructure of the rejuvenated superalloy

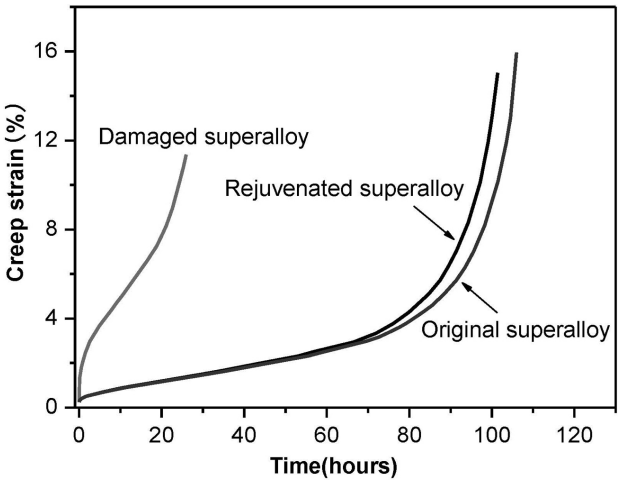

Figure 6: Creep curves for the original, damaged and rejuvenated superalloy at 980 °C and 190 MPa

and the size of fine γ' precipitates is smaller than that of the γ' precipitates obtained after heat-treatment cycle C. In fact, the aging temperature of 1121 °C is below the temperature of the γ' precipitate dissolution in the DZ411 superalloy. So, it is concluded that the obtained coarse γ' precipitates were derived due to the growth of the secondary γ' precipitates, which formed during the cooling after the solution treatment and the fine ones are tertiary γ' precipitates which reprecipitated during the aging treatment.

This kind of γ' precipitate microstructure is expected and theoretically desired as the most optimized microstructure that can provide for very good high-temperature properties. **Figure 6** shows creep curves for the original, damaged and rejuvenated superalloy at 980 °C and 190 MPa. It is evident that the creep curve of the DZ411 superalloy after heat-treatment cycle I is remarkably similar to that of the original superalloy. Moreover, the creep-rupture time of the rejuvenated superalloy is near to that of the original superalloy, but about four times longer than that of the damaged superalloy. Therefore, it is feasible to restore the microstructure and creep properties of directionally solidified DZ411 superalloy with a simple re-heat rejuvenation treatment.

4 CONCLUSIONS

A creep-damaged DZ411 superalloy was initially obtained with an interrupted creep test. The damaged superalloy was then subjected to different solution-treatment cycles and a two-step aging treatment to reveal the influences of different solution conditions on γ' precipitate characteristics and investigate the evolution of degenerated γ' characteristics. Based on the observations and analysis results, the following conclusions were obtained:

1. The creep test gave rise to a microstructural degradation of the original superalloy. The microstructural de-

terioration was evidenced mainly by the coarsening and rafting of prime γ' precipitates and disappearance of secondary γ' precipitates.

2. Proper solution conditions including 1220 °C and 2 h provide for a dissolution of the coarsened and rafted prime γ' precipitates and reprecipitation of fine secondary γ' precipitates during the cooling process after the solution treatment, while avoiding incipient melting during the re-heat rejuvenation treatment of the damaged superalloy.

3. Solution treatment at a higher temperature results in a smaller size and higher volume fraction of the γ' precipitates. However, solution treatment at a longer holding time produces a larger size and a lower volume fraction of the γ' precipitates. High cooling rates after the solution treatment give rise to finer and more secondary γ' precipitates.

4. A complete rejuvenation procedure including a full solution and two-step aging can produce a duplex-sized γ' precipitate microstructure with coarse cubic γ' precipitates and fine spherical γ' precipitates, providing very good high-temperature creep properties.

5. It is verified that the microstructure and creep properties of the creep-damaged DZ411 superalloy can be restored with a simple re-heat rejuvenation treatment.

Acknowledgment

This paper was supported by the National Natural Science Foundation of China (No. 51601145).

5 REFERENCES

[1] J. Wang, L. Z. Zhou, L. Y. Sheng, J. T. Guo, The microstructure evolution and its effect on the mechanical properties of a hot-corrosion resistant Ni-based superalloy during long-term thermal exposure, Materials and Design, 39 (**2012**) 1, 55–62, doi:10.1016/j.matdes.2012.02.020

[2] F. Sun, J. Y. Tong, Q. Feng, J. X. Zhang, Microstructural evolution and deformation features in gas turbine blades operated in-service, Journal of Alloys and Compounds, 618 (**2015**) 5, 728–733, doi:10.1016/j.jallcom.2014.08.246

[3] E. Lvova, A comparison of aging kinetics of new and rejuvenated conventionally cast GTD-111 gas turbine blades, Journal of Materials Engineering and Performance, 16 (**2007**) 2, 254–264, doi:10.1007/s11665-007-9046-y

[4] Y. Yoshioka, D. Saito, R. Takaku, S. Itou, I. Sato, K. Ishibashi, Y. Sakai, Development, reliability evaluation and service experiences of gas turbine blade life regeneration technology, Transactions of the Indian Institute of Metals, 63 (**2010**) 2–3, 289–295, doi:10.1007/s12666-010-0039-4

[5] S. S. Hosseini, S. Nategh, A. A. Ekrami, Microstructural evolution in damaged IN738LC alloy during various steps of rejuvenation heat treatments, Journal of Alloys and Compounds, 512 (**2012**) 1, 340–350, doi:10.1016/j.jallcom.2011.09.094

[6] T. Y. Wang, X. M. Wang, Z. H. Zhao, Z. Zhang, Effect of HIP combined with RHT process on creep damage of DZ125 superalloy, Journal of Materials Engineering, 45 (**2017**) 2, 88–95, doi:10.11868/j.issn.1001-4381.2014.001203

[7] A. Turazi, C. A. S. Oliveir, C. E. N. Bohórquez, F. W. Comeli, Study of GTD-111 superalloy microstructural evolution during high-temperature aging and after rejuvenation treatments, Metallography, Microstructure and Analysis, 4 (**2015**) 1, 3–12, doi:10.1007/s13632-014-0177-x

[8] G. Van Drunen, J. Liburdi, Rejuvenation of used turbine blades by hot isostatic pressing, Turbomachines, (**1977**), 55–60, doi:10.21423/R1MQ1G

[9] P. Wangyao, V. Krongtong, N. Panich, N. Chuankrerkkul1, G. Lothongkum, Effect of 12 heat treatment conditions after HIP process on microstructural refurbishment in cast nickel-based superalloy GTD-111, High Temperature Materials and Processes, 26 (**2007**) 2, 151–160, doi:10.1515/HTMP.2007.26.2.151

[10] A. K. Koul, J. P. Immarigeon, R. Castillo, P. Lowden, J. Liburdi, Rejuvenation of service-exposed IN-738 turbine blades, Superalloys, (**1988**), 755–764, doi:10.7449/1988/Superalloys-1988-755-764

[11] D. L. Klarstrom, G. L. Hoback, V. R. Ishwar, J. I. Qureshi, Rejuvenation heat treatment and weld repairability studies of Haynes 230 alloy, Proceedings of ASME Turbo Expo: Power for Land, Sea and Air, (**2000**), doi:10.1115/2000-GT-0629

[12] Y. Yoshioka, Y. Yoshioka, D. Saito, K. Ishibashi, J. Ishii, A. Izumi, Life-refurbishment of service-degraded gas turbine buckets, Proceedings of ASME Turbo Expo: Power for Land, Sea and Air, (**2004**), doi:10.1115/GT2004-54040

[13] H. R. Tipler, M. Mclean, Assessment of damage accumulation and property regeneration by hot isostatic pressing and heat treatment of laboratory-tested and service exposed IN738LC, Superalloys, (1984), 73–82, doi:10.7449/1984/Superalloys-1984-73-82

[14] H. M. Tawancy, L. Al-Hadhrami, On the service performance of refurbished turbine blades in a power station, Proceedings of ASME Turbo Expo: Power for Land, Sea and Air, (**2008**), 407–413, doi:10.1115/GT2008-50057

[15] A. James, Review of rejuvenation process for nickel base superalloys, Materials Science and Technology, 17 (**2001**) 5, 481–486, doi:10.1179/026708301101510168

[16] J. Liburdi, P. Lowden, D. Nagy, T. Rusan, D. Priamus, S. Shaw, Practical experience with the development of superalloy rejuvenation, Proceedings of ASME Turbo Expo: Power for Land, Sea and Air, (**2009**) 4, 819–827, doi:10.1115/GT2009-59444

[17] X. M. Wang, Y. Zhou, Z. H. Zhao, Z. Zhang, Morphological evolution of γ' precipitate under various rejuvenation heat treatment cycles in a damaged nickel-based superalloy, Rare Metals, (**2016**) 1–6, doi:10.1007/s12598-015-0687-y

[18] S. A. Sajjadi, S. M. Zebarjad, R. I. L. Guthrie, M. Isac, Microstructure evolution of high-performance Ni-base superalloy GTD-111 with heat treatment parameters, Journal of Materials Processing Technology, 175 (**2006**) 376–381, doi:10.1016/j.jmatprotec.2005.04.021

[19] Y. Zhou, Z. Zhang, Z. Zhao, Q. P. Zhong, Effects of HIP temperature on the microstructural evolution and property restoration of a Ni-based superalloy, JMEPEG, 22 (**2013**) 1, 215–222, doi:10.1007/s11665-012-0246-8

[20] P. Wangyao, V. Krongtong, N. Panich, Effect of 12 heat treatment conditions after HIP process on microstructural refurbishment in cast nickel-based superalloy, GTD-111, High Temperature Material Processes, 26 (**2007**) 2, 151–159, doi:10.1515/HTMP.2007.26.2.151

[21] B. Ruttert, D. Burger, L. M. Roncery, Rejuvenation of creep resistance of a Ni-base single-crystal superalloy by hot isostatic pressing, Materials and Design, 134 (**2017**) 1, 418–425, doi:10.1016/j.matdes.2017.08.059

[22] L. H. Rettberg, M. Tsunekane, T. M. Pollock, Rejuvenation of nickel-based superalloys GTD 444 (DS) and RENE N5 (SX), Superalloys, (**2012**) 341–349, doi:10.7449/2012/Superalloys-2012-341-349

[23] H. S. Lee, D. H. Kim, D. S. Kim, K. B. Yoo, Microstructural changes by heat treatment for single crystal superalloy exposed at high temperature, Journal of Alloys and Compounds, 561 (**2013**) 135–141, doi:10.1016/j.jallcom.2013.01.129

[24] J. Zhang, L. Lou, H. Li, Material and processing technology of directionally solidified blade in heavy duty industrial gas turbines, Acta Metallurgica Sinica, 32 (**2013**), 12–38, doi:10.7502/j.issn.1674-3962.2013.01.02

[25] J. Zhang, J. Shen, Y. Z. Lu, L. H. Lou, Processing, microstructure and mechanical properties of large directionally solidified castings for industrial gas turbine applications, Materials China, 46 (**2010**), 1322–1326, doi:10.3724/SP.J. 1037. 2010.00509

[26] A. Baldan, Review Progress in Ostwald ripening theories and their applications to nickel-base superalloys, Part I: Ostwald ripening theories, Journal of Materials Science, 37 (**2002**) 11, 2171–2202, doi:10.1023/A:1015388912729

[27] T. Grosdidier, A. Hazotte, A. Simon, Precipitation and dissolution processes in γ/γ' single crystal nickel-based superalloys, Materials Science and Engineering A, 256 (**1998**) 1, 183, doi:10.1007/s12598-015-0687-y

[28] N. El-Bagoury, M. Waly, A. Nofal, Effect of various heat treatment conditions on microstructure of cast polycrystalline IN738LC alloy, Materials Science and Engineering A, A487 (**2008**) 1–2, 152–161, doi:10.1016/j.msea.2007.10.004